Biomaterials 35 (2014) 2798–2808

Contents lists available at ScienceDirect

Biomaterials

journal homepage: www.elsevier.com/locate/biomaterials

The effect of cyclic stretch on maturation and 3D tissue formation of human embryonic stem cell-derived cardiomyocytes

Anton Mihic [a], Jiao Li [a,1], Yasuo Miyagi [a], Mark Gagliardi [b], Shu-Hong Li [a], Jean Zu [d], Richard D. Weisel [a,b], Gordon Keller [b,c], Ren-Ke Li [a,b,*]

[a] Division of Cardiovascular Surgery and Toronto General Research Institute, University Health Network and Department of Surgery, Division of Cardiac Surgery, University of Toronto, Toronto, ON, Canada
[b] McEwen Centre for Regenerative Medicine, Toronto, ON, Canada
[c] Department of Medical Biophysics, University of Toronto, Toronto, ON, Canada
[d] Department of Mechanical and Industrial Engineering, University of Toronto, Toronto, ON, Canada

ARTICLE INFO

Article history:
Received 29 October 2013
Accepted 19 December 2013
Available online 11 January 2014

Keywords:
Cardiac tissue engineering
Cardiomyocyte
Human embryonic stem cell
Scaffold
Transplantation
Uniaxial stretch

ABSTRACT

The goal of cardiac tissue engineering is to restore function to the damaged myocardium with regenerative constructs. Human embryonic stem cell–derived cardiomyocytes (hESC-CMs) can produce viable, contractile, three-dimensional grafts that function *in vivo*. We sought to enhance the viability and functional maturation of cardiac tissue constructs by cyclical stretch. hESC-CMs seeded onto gelatin-based scaffolds underwent cyclical stretching. Histological analysis demonstrated a greater proportion of cardiac troponin T–expressing cells in stretched than non-stretched constructs, and flow sorting demonstrated a higher proportion of cardiomyocytes. Ultrastructural assessment showed that cells in stretched constructs had a more mature phenotype, characterized by greater cell elongation, increased gap junction expression, and better contractile elements. Real-time PCR revealed enhanced mRNA expression of genes associated with cardiac maturation as well as genes encoding cardiac ion channels. Calcium imaging confirmed that stretched constructs contracted more frequently, with shorter calcium cycle duration. Epicardial implantation of constructs onto ischemic rat hearts demonstrated the feasibility of this platform, with enhanced survival and engraftment of transplanted cells in the stretched constructs. This uniaxial stretching system may serve as a platform for the production of cardiac tissue-engineered constructs for translational applications.

1. Introduction

Tissue engineering offers the promise to replace damaged myocardial tissue after injury [1]. Biodegradable scaffolds seeded with stem cells may restore ventricular function after a myocardial infarction (MI), particularly if the seeded cells become mature cardiomyocytes that can be induced to beat synchronously with the heart.

A number of cell types have been evaluated in the clinical context of cardiac repair [2,3]; however, most have not formed functioning cardiomyocytes. Embryonic stem cells have the capability to become functioning cardiomyocytes and may be the ideal cell source for cardiac regeneration [4]. However, injecting dissociated cells into the injured myocardium can induce anoikis [5] and markedly reduces the functionality of the cardiomyocytes [6]. Expanding human embryonic stem cell–derived cardiomyocytes (hESC-CMs) in a three-dimensional (3D) collagen scaffold permits the delivery of the intact construct to the heart. Although cell sheets avoid the use of foreign materials [7], thicker and porous cell-seeded scaffolds provide a better microenvironment for cardiomyocyte maturation [8,9]. A comparison of the epicardial placement of cell sheets and a cell-seeded collagen scaffold found that both similarly improved ventricular function after an MI [10]. In previous studies, we found that cell-seeded synthetic biodegradable scaffolds improved heart function [11,12], but the collagen scaffold provided the best milieu for beating cardiomyocytes [13].

To adequately contribute to the restoration of cardiac function, cell-seeded constructs need to function as mature rather than fetal cardiomyocytes [4,14,15]. hESC-CMs have a markedly immature phenotype as defined by their morphology, gap junction expression, contractile apparatus, spontaneous automaticity, and electrophysiological and calcium handling properties [16]. Cardiomyocyte maturation can be achieved through multiple

* Corresponding author. MaRS Centre, Toronto Medical Discovery Tower, Room #3-702, 101 College St., Toronto, ON, Canada M5G 1L7. Tel.: +1 416 581 7492; fax: +1 416 581 7493.
E-mail address: renkeli@uhnres.utoronto.ca (R.-K. Li).
[1] Present address: Department of Cardiology, The Second Affiliated Hospital of Guangzhou Medical College, Guangzhou, Guangdong, China.

0142-9612/$ – see front matter © 2014 Elsevier Ltd. All rights reserved.
http://dx.doi.org/10.1016/j.biomaterials.2013.12.052

stimuli, including electrical stimulation [17–19], mechanical stretching [17,20–22], construct stiffness and topology [18,23], and chemical manipulation [15,22]. Maturation of hESC-CM–seeded scaffolds *in vitro*, prior to their transplantation, will enhance 3D tissue formation by stimulating diffusion within the construct and cellular hypertrophy.

In the current study, we evaluated the effects of uniaxial cyclic stretch [24], which facilitated the expansion and maturation of hESC-CM–seeded scaffolds [25,26]. The *in vivo* feasibility of epicardial implantation of the cell-seeded scaffolds was evaluated in nude rats using a cardiac ischemia/reperfusion (I/R) model.

2. Materials and methods

A complete description of the methods is included in the Online Supplement.

2.1. Cardiac specification and cell culture

The HES2 human embryonic stem cell line (NIH code ES02; ES Cell International) was maintained and directed toward cardiovascular lineages as previously described [25–27], with cytokines BMP4, bFGF, and activin A in a stage-specific manner. Embryoid bodies were disassociated into a single-cell suspension for seeding onto scaffolds. The proportion of troponin T (TnT) positive cells as determined by flow cytometric analyses ranged from 40% to 50% for each preparation. The disassociated cells are referred to as hESC-CMs.

2.2. Construct preparation and uniaxial stretching

Absorbable gelatin sponges (Gelfoam, Ethicon) were cut into 30 × 10 × 7 mm strips, presoaked in medium, and evenly seeded with 6×10^6 hESC-CMs on their surface. Following the initial 48 h period, constructs were divided into two groups: a static culture condition (control) and a stretching culture condition in which constructs were uniaxially cycled between stretched and relaxed states. A custom-built stretching apparatus using a non-contact electromagnetic force applied to stainless steel clamps fixed to either end of the construct was utilized as previously described [24]. The uniaxial stretching program controlled the extent, frequency, pattern, and duration of stretch. Cyclical stretching was performed with a displacement of approximately 12%, a frequency of 1.25 Hz (75 cycles/min), and continuous cycling with each "stretch" comprising 37% of the cycle duration. Stretched constructs were cultured under these conditions for 72 h, and control constructs remained under static, but otherwise identical, culture conditions. This procedure is summarized in Fig. S1.

2.3. Calcium imaging

Constructs were incubated with 5 μM of the calcium-sensitive dye Fluo-4 AM (Life Technologies) according to the manufacturer's instructions. Constructs were washed with fresh Tyrode solution, and calcium transients were recorded using confocal imaging. Rapid stacking of sequential line scans over 30 s produced data that corresponded to a group of neighboring cells spontaneously contracting. Four different constructs were examined for each group, with 6–10 areas studied per construct. Whole-frame images obtained at 128 × 128 pixels were continuously recorded to produce short video sequences. Both sets of data were analyzed using ImageJ software (NIH).

Supplementary video related to this article can be found online at http://dx.doi.org/10.1016/j.biomaterials.2013.12.052.

2.4. Animal studies

The Animal Care Committee of University Health Network approved all animal studies. Male RNU-Nude rats (02N01, National Cancer Institute) weighing ~200 g were used for *in vivo* studies. One week before construct implantation, I/R injury was produced by temporarily ligating the anterior descending coronary artery for 45 min. Constructs (~7.0 × 8.0 × 3.5 mm) were surgically attached to the surface of the lateral ventricular free wall, with the top surface placed in contact with the epicardium. Animals were monitored for 2 weeks.

2.5. Statistics

All data are presented as mean ± SEM and analyzed using unpaired *t*-tests or one-way or two-way analysis of variance (ANOVA) where appropriate. A value of $p < 0.05$ was considered statistically significant.

3. Results

3.1. Preparation of cardiac tissue constructs

To establish the optimal number of cells to produce tissue constructs, we tested three doses of hESC-CMs seeded onto control (non-stretched) Gelfoam (Fig. 1A–C). Histological analysis revealed a roughly linear relationship between the number of seeded cells and the expression of cardiomyocyte-specific TnT (Fig. 1B). Furthermore, the relative number of proliferating cells at each dose remained constant as determined by the incorporation of bromodeoxyuridine (BrdU; Fig. 1C). Therefore, we chose to seed the constructs with 6×10^6 cells, consistent with our ability to scale hESC-CM production to achieve an even distribution of cells within the construct.

Cells were evenly seeded onto the surface of Gelfoam constructs and allowed to adhere for 48 h. Constructs that underwent cyclical stretching were stimulated at a frequency of 1.25 Hz with approximately 12% length displacement. The duty cycle, the duration of active contraction or relaxation during one cycle, was 37%. Rhythmic, uniaxial stretching was achieved using non-contacting electromagnetic driving forces that simultaneously displaced the construct at both ends (Fig. 1D). Control constructs did not undergo stretching.

3.2. Construct characterization

Histological analysis of non-stretched constructs revealed dense seeding at the surface, but more sparse cell seeding at distances from the surface, as we reported previously with isolated human heart cells [21]. Fig. 1E shows that stretching improved the dispersion of cells throughout the biomaterial at depths perpendicular to the top surface of the construct.

Scanning electron microscopy (SEM) was used to evaluate the structure of the constructs (Fig. 1F, Fig. S2). At lower magnifications, there was no apparent difference between control and stretched constructs in terms of pore size, shape, or degradation. However, at higher magnifications, the cells in the stretched constructs were more elongated and less clustered.

Immunostaining demonstrated that stretched constructs stained more strongly for cardiomyocyte-specific TnT and exhibited striations with Z-bands running longitudinally along the hESC-CMs (Fig. 2A; $p < 0.05$). Western blotting showed that stretched constructs expressed more TnT than control constructs (Fig. 2B; $p < 0.05$).

Cyclic stretching improved diffusion within the porous Gelfoam matrix, providing better oxygen and nutrient concentrations for cells while also providing environmental mechanical cues for hESC-CMs. Therefore, we performed flow cytometry on an equal number of cells disassociated from both types of constructs and assessed TnT expression. As shown in Fig. 2C, stretched constructs contained a significantly higher proportion of TnT-expressing cardiomyocytes (44.0 ± 0.3% vs. 26.2 ± 0.3%, $p < 0.01$). To further confirm the identity of these cells as cardiomyocytes, and to isolate these cardiomyocytes for later analysis, we employed an NKX2-5-GFP reporter hESC line (Fig. 2D) [28]. Flow cytometric analyses revealed that stretched constructs contained a higher proportion of NKX2-5-GFP^+/CD90-APC^- cardiomyocytes versus control constructs (29.8 ± 1.5% vs. 23.5 ± 0.4%, $p < 0.05$).

3.3. hESC-Cm ultrastructure

To further characterize cell morphology, we examined the hESC-CM ultrastructure with transmission electron microscopy (TEM). Control hESC-CMs appeared smaller and more clustered than stretched cells, which were more elongated and larger (Fig. 3A). Furthermore, stretched constructs contained more contractile proteins, indicated by the striated structures running longitudinally in the elongated cells (Fig. 3B). These striated structures had well defined Z-bands, which in some cases crossed neighboring plasma membranes and spanned multiple cells. Stretched constructs exhibited more gap junctions between neighboring plasma membranes (Fig. 3C), suggesting enhanced connexin expression.

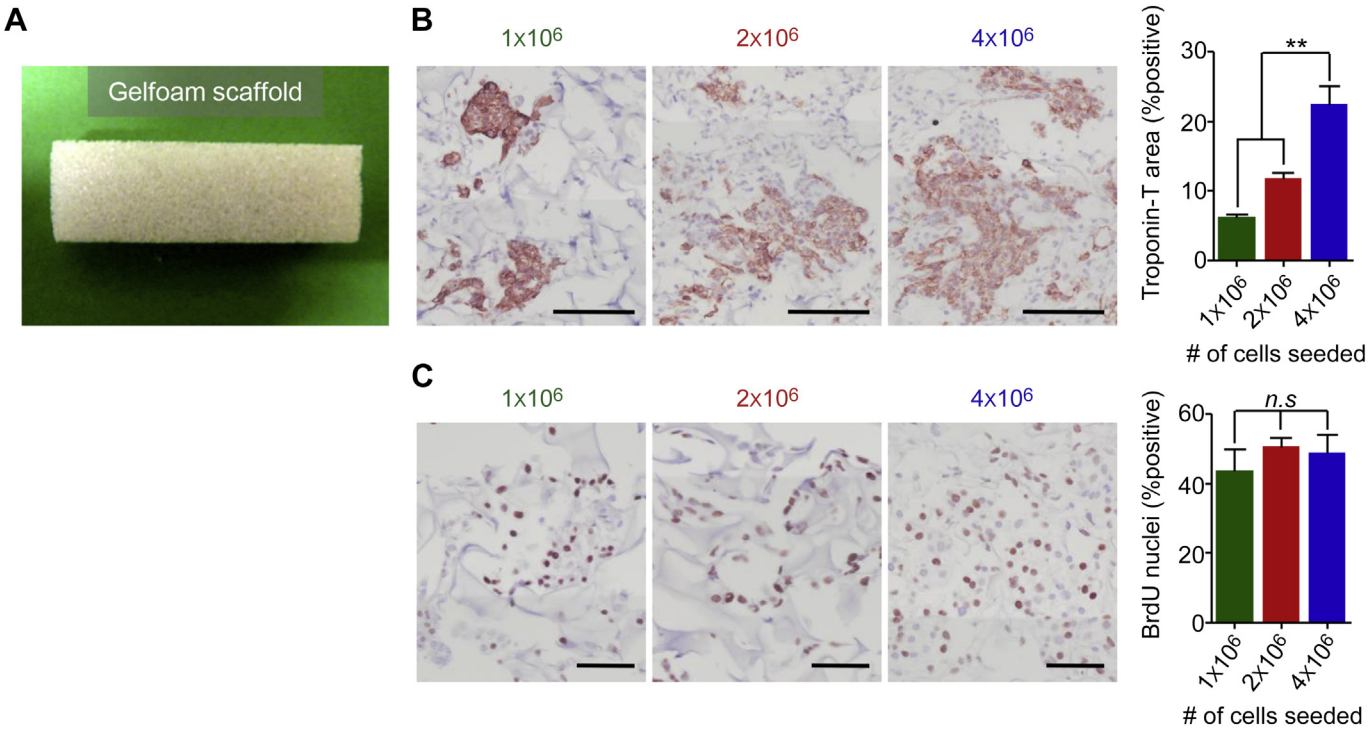

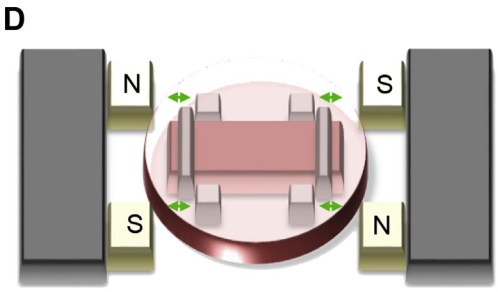

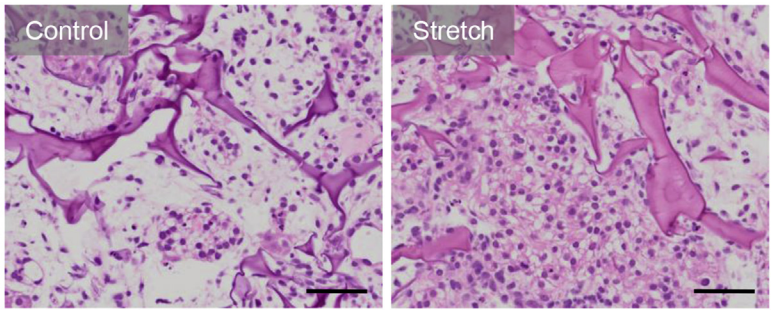

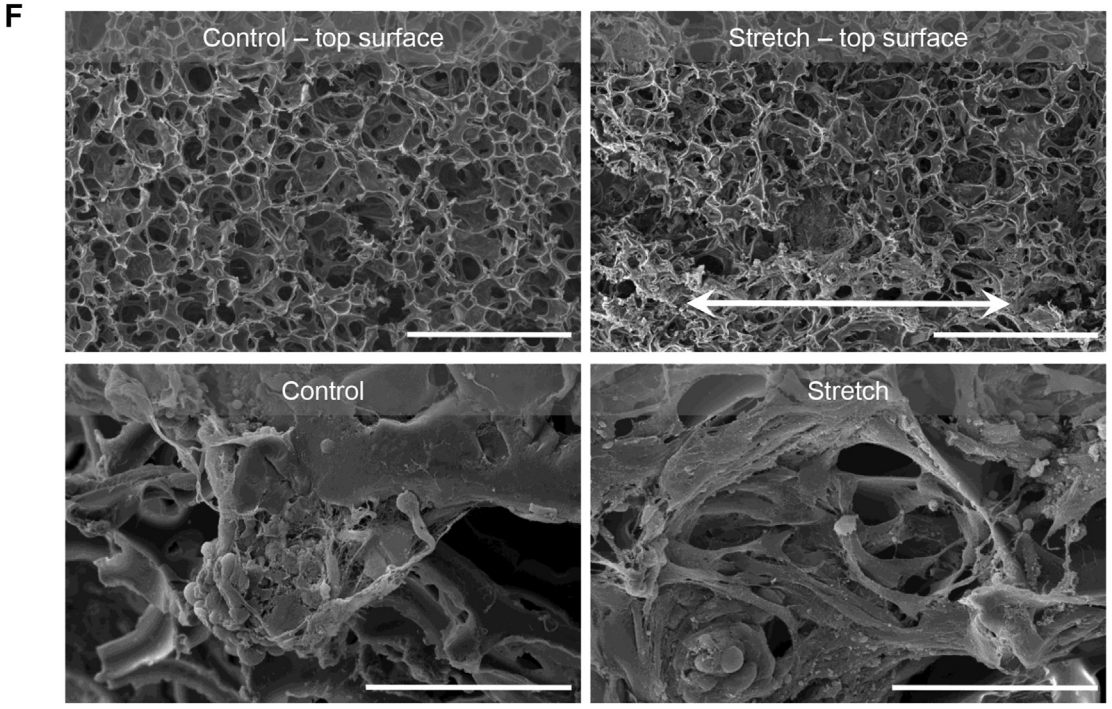

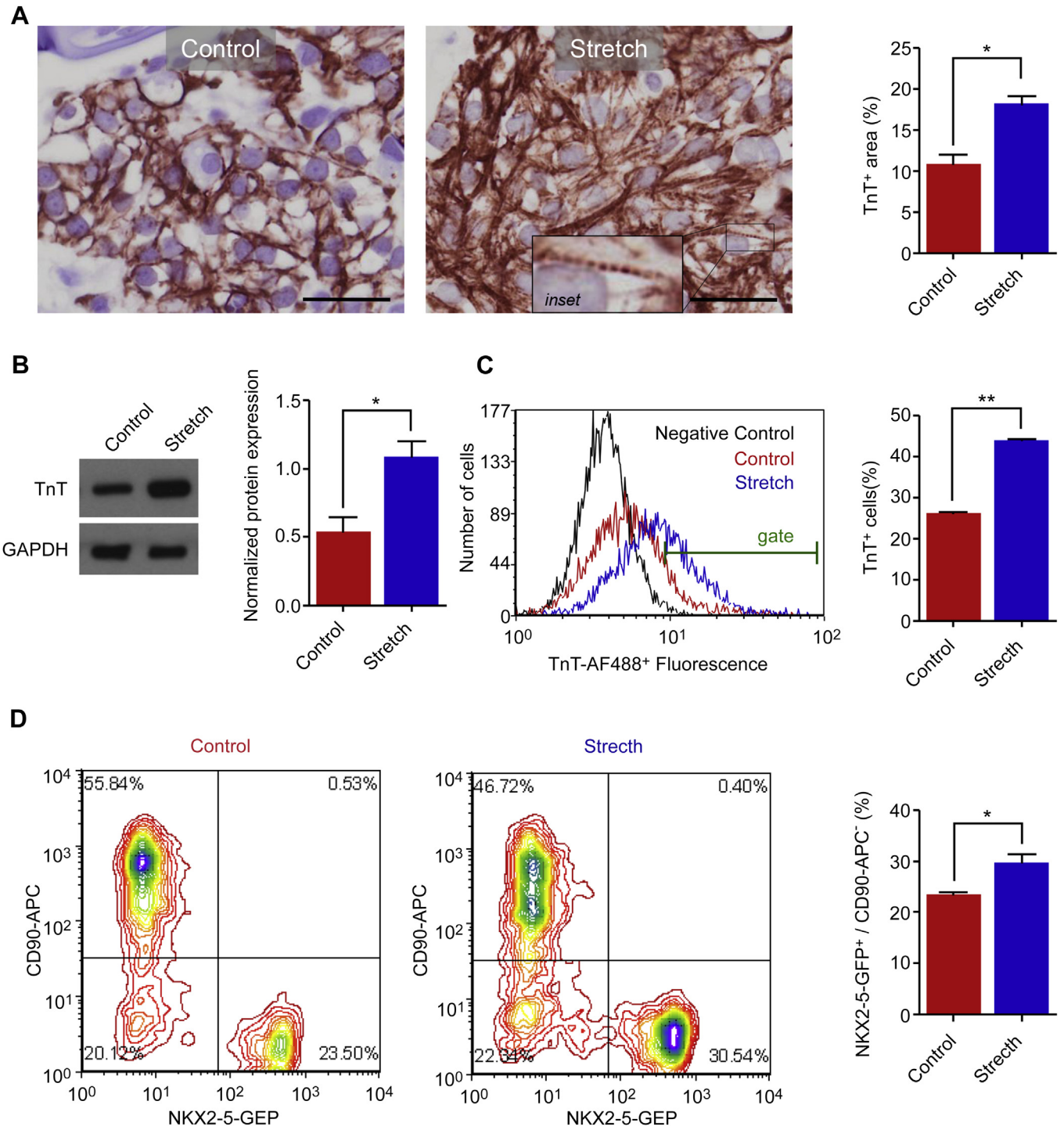

Fig. 2. Stretched constructs contained a larger proportion of cardiomyocytes. (A) Immunostaining for TnT demonstrated greater expression in stretched constructs and well-defined striations with Z-banding running longitudinally along the stretched hESC-CMs (inset) (scale bar 25 μm; $n = 4$/group). (B) Western blot showed that stretched constructs expressed more TnT protein than control constructs ($n = 3$/group). (C) The total population of cells disassociated from scaffolds were labeled with TnT and flow sorted, revealing a larger proportion of TnT-expressing cells in stretched constructs. The negative control consisted of disassociated cells without primary antibody ($n = 4$/group). (D) Flow assisted cell sorting (FACS) confirmed that the proportion of NKX2-5-GFP$^+$/CD90-APC$^-$ cardiomyocytes was higher in stretched than in control constructs ($n = 3$/group). $^*p < 0.05$, $^{**}p < 0.01$.

Fig. 1. Stretched constructs contained better dispersed and elongated cardiomyocytes. (A) Gelfoam scaffold. (B&C) Optimization of cell-seeding concentration. A roughly linear increase in the number of TnT-positive cardiomyocytes was observed up to 4×10^6 cells/scaffold (B, $n = 4$/group, scale bar 100 μm). There was no change in the proportion of BrdU-positive proliferating nuclei (C, $n = 4$/group, scale bar 50 μm). (D) The stretching apparatus exerted non-contact electromagnetic forces, simultaneously displacing the construct at both ends. N = north pole, S = south pole of magnets. (E) Cross-sectional hematoxylin and eosin staining showed better dispersion of cells in stretched constructs. Cyclical stretching produced fewer cell aggregates (scale bar 50 μm). (F) SEM showed no difference in pore size or directionality in the constructs (top panels, arrow denotes axis of uniaxial stretch, scale bar 1 mm). However, cells in the stretched constructs were elongated and less clustered (bottom panels, scale bar 100 μm). $^{**}p < 0.01$, *n.s.* = not significant.

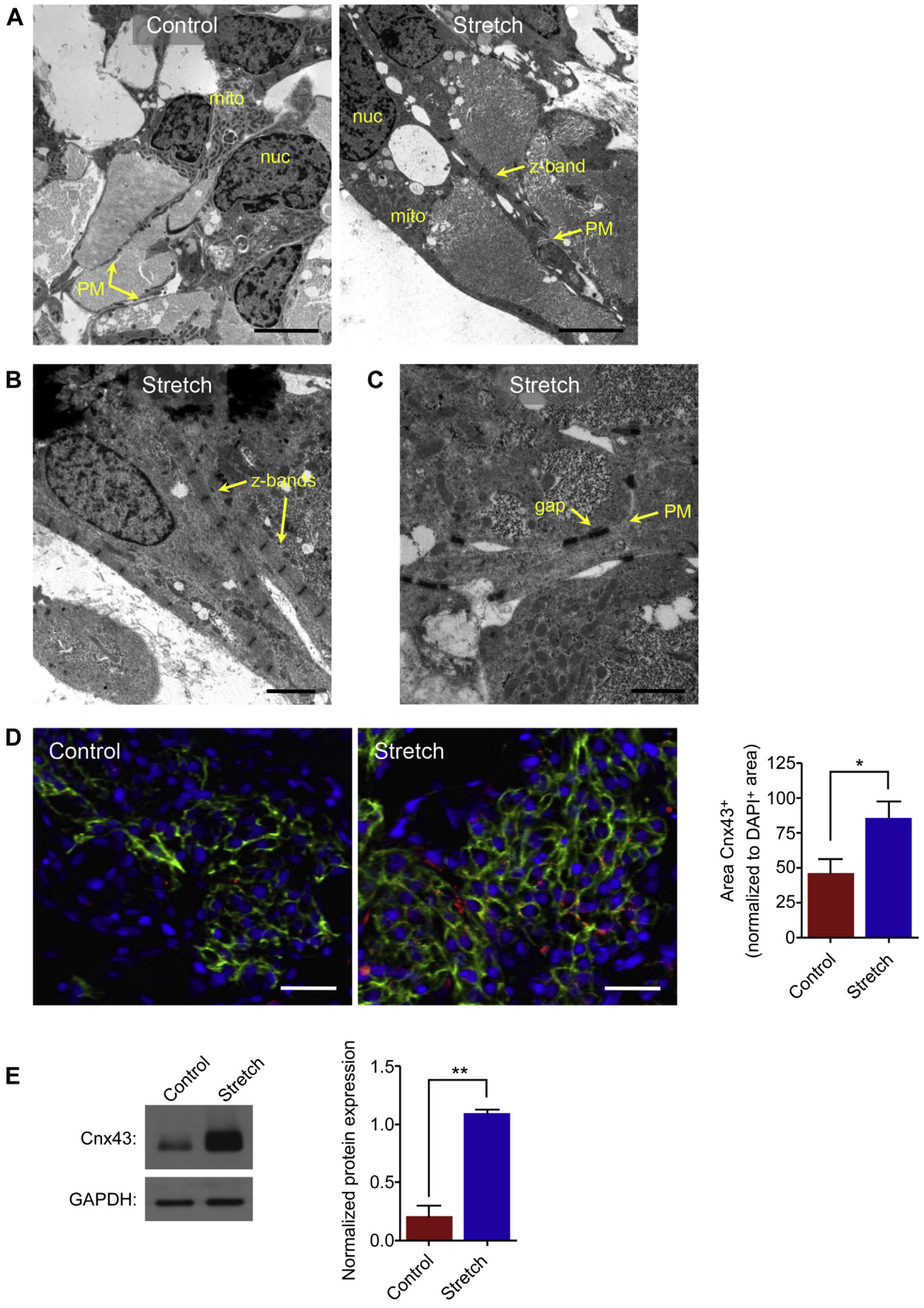

To confirm the increased expression of gap junction proteins, we immunostained for connexin 43 (Cnx43), the most predominant connexin in the human heart. TnT expression was used as a positive marker for cardiomyocytes, and Cnx43 expression was normalized DAPI-positive nuclei for whole construct cross-sections. Stretched constructs expressed significantly higher levels of Cnx43 versus control (Fig. 3D; $p < 0.01$). The expression of Cnx43 protein in whole construct lysates was confirmed using Western blot (Fig. 3E; $p < 0.01$).

3.4. hESC-Cm function

hESC-CM function within the constructs was examined using calcium imaging. Spontaneous calcium oscillations were captured using time-lapsed confocal microscopy (Fig. 4A, Video S1). Regions of interest (ROIs) were selected, and the averaged signal intensity for that ROI was normalized to the maximum fluorescence after subtracting baseline. Spontaneous calcium transients occurred nearly simultaneously in neighboring cells of both groups, indicating that cells were electrically coupled. Use of high-speed line scanning (Fig. 4B), in which single one-dimensional pixel scans were stacked consecutively over time, allowed for the quantitative analysis of calcium transients. Simultaneous calcium waves were demonstrated in both groups. However, the stretched constructs cycled calcium faster than control (Fig. 4C; 70.5 ± 7.1 cycles/min vs. 36.4 ± 1.9 cycles/min, $p < 0.05$). In addition, the duration of each calcium cycle, an indicator of the time required to restore intracellular calcium to normal resting levels, was quantified. Control constructs had longer calcium cycle durations compared to stretched constructs (Fig. 4D and 0.70 ± 0.04 s vs. 0.50 ± 0.07 s, $p < 0.05$). These results demonstrate that stretched constructs have a higher spontaneous beating frequency, approaching that of the stretching induction protocol (1.25 Hz), and the cells were able to cycle intracellular calcium more rapidly to achieve this faster beating frequency.

3.5. Stretch-induced changes in hESC-CM ion channel expression

Mature cardiomyocytes express high levels of cardiac-specific ion channels, which facilitate the propagation of cardiac action potentials (APs) and initiate myocyte contraction. We evaluated transcript levels of several cardiac ion channel genes using quantitative real-time PCR in FACS isolated NKX2-5-GFP$^+$/CD90-APC$^-$ cardiomyocytes following dissociation from the constructs (Fig. 4E). An important determinant of AP depolarization and duration is the L-type voltage-gated calcium channel (CaV1.2; *CACNA1C*). Expression of this channel increased 4.90-fold in stretched constructs relative to control constructs. The sodium/potassium hyperpolarization-activated cyclic nucleotide-gated channel (*HCN4*), which is responsible for the spontaneous pacemaker currents produced by the sinoatrial node, was unchanged. The delayed-rectifier voltage-gated potassium hERG channel (Kv11.1; *KCNH2*), which is important for cardiac repolarization, was moderately upregulated 1.48-fold. Expression of the voltage-gated sodium channel Nav1.5 (*SCN5A*) was upregulated 5.25-fold, and the inward-rectifier potassium channel Kir2.1 (*KCNJ2*) was upregulated 3.23-fold. However, we did not observe a change in the transcript levels of the slowly activating delayed rectifier potassium channel KvLQT1 (Kv7.1; *KCNQ1*), a mediator of cardiac repolarization.

3.6. Stretch-induced changes in hESC-CM gene and protein expression

During human cardiomyocyte maturation, a number of transcription levels change. We examined the expression of several genes known to be indicative of cardiomyocyte maturity in FACS isolated NKX2-5-GFP$^+$/CD90-APC$^-$ cardiomyocytes using quantitative real-time PCR (Fig. 5A). Furthermore, we examined cell lysates from whole constructs which are composed of a heterogeneous population of hESC-CMs, using Western blotting (Fig. 5B). The direct comparison of protein expression from the heterogeneous constructs and gene expression of FACS isolated cardiomyocytes is problematic due to the protein expression profiles of the non-myocyte fractions. Cardiac-specific α- and β-myosin heavy chain (MHC) are robustly expressed throughout the human myocardium. In early development, the energy-efficient α-isoform predominates. Throughout adult life, the β-isoform is more robustly expressed. Stretching did not alter the mRNA expression of the α-MHC isoform (*MYH6*), but there was a significant increase in the expression of β-MHC (*MYH7*; 2.00-fold). We found no difference in protein expression for total α/β-MHC. Gene expression of myosin light chain-2V (ventricular specific; *MLC-2V*) and α-cardiac actin (*ACTC1*) mRNA was unchanged; however, stretched constructs did possess higher protein expression of these factors from total construct cell lysates.

Furthermore, the mRNA level of the transcription factor MEF-2C, important for early cardiogenesis and vasculogenesis, was significantly reduced in stretched hESC-CMs relative to control (*MEF2C*; 0.57-fold expression), which corresponded to a significant reduction in the protein expression in stretched constructs. We also investigated the expression of atrial natriuretic peptide (ANP), which has a role during heart development but gradually declines in expression during adulthood. Interestingly, we observed an increase in ANP gene expression in stretched sorted cardiomyocytes (*NPPA*; 2.62-fold), but total protein expression from total construct cell lysates was lower in the stretched versus control group. Taken together, the gene expression results are in agreement with previous studies demonstrating that uniaxial stretching upregulates the expression of β-MHC and ANP [20]; however, the protein data suggests that, as a whole, stretched constructs had undergone some degree of physical maturation as they expressed higher levels of MLC-2V and α-cardiac actin, with reduced expression of MEF-2C and ANP protein.

3.7. Feasibility of stretched constructs for in vivo cardiac repair

To assess the potential of these constructs to improve the function of injured hearts *in vivo*, we utilized a rat model of I/R injury. We tested control (non-stretched), stretched, and acellular non-stretched constructs by implanting them on the epicardial surface over the injured left ventricular free wall 7 days after I/R. Constructs were trimmed to 8×7 mm (Fig. 6A) and were sutured onto the epicardium with one stitch at each corner of the construct. Two weeks after implantation, the constructs were intact and clearly visible (Fig. 6B).

At this time, an 8-lead (octapolar) catheter was used to simultaneously measure the electrical characteristics of the epicardium and the surface of the construct. Electrode pairs were separated by a distance of 4.5 mm and were placed along the myocardium with a

Fig. 3. hESC-CM ultrastructure and Cnx43 expression were enhanced in stretched constructs. (A) TEM showed smaller and more clustered control hESC-CMs and elongated and larger stretched cells (scale bar 4 μm). (B) Stretched cells exhibited more striated structures running longitudinally along the cells, spaced approximately 1.5–2 μm apart, with Z-bands spanning multiple cells (inset; scale bar 2 μm). (C) Stretched constructs had more gap junctions between neighboring plasma membranes (scale bar 1 μm). (D) Immunostaining and quantification of Cnx43 (red) normalized to DAPI (blue) expression showed stretched constructs expressed higher levels of Cnx43 than control constructs ($n = 4$/group, scale bar 40 μm; TnT immunostained in green). (E) Western blotting confirmed greater Cnx43 protein expression in stretched constructs ($n = 3$/group). mito = mitochondria, nuc = nucleus, PM = plasma membrane, gap = gap junction. $^*p < 0.05$, $^{**}p < 0.01$.

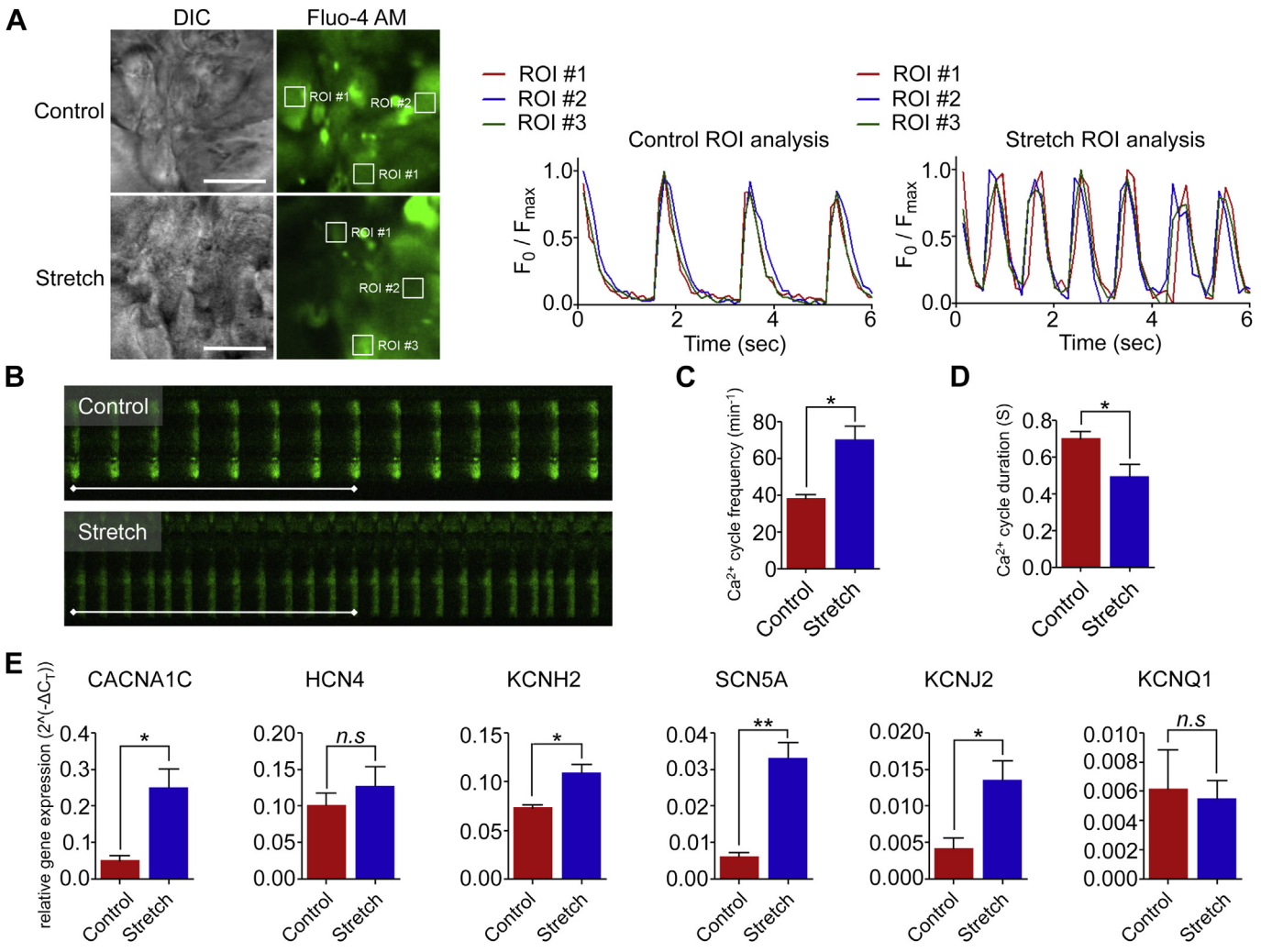

Fig. 4. Calcium imaging revealed faster spontaneous contractions in stretched constructs. (A) Non-confocal differential interference contrast (DIC) and time-lapse averaged Fluo-4 AM images from control and stretched constructs were analyzed by selecting multiple ROIs and plotting the average intensity (F_{max}/F_o) for each ROI over time. These studies demonstrated that multiple neighboring cells contracted spontaneously and were electrically coupled as peak calcium transients occurred nearly simultaneously (scale bar 20 μm). (B) Line scanning across multiple cells (>5) captured spontaneous calcium oscillations in both stretched and control constructs (10 replicates of each construct were averaged to represent 1 independent experiment; scale bar denotes 10 s of stacked line scans). (C) Analysis of line scans demonstrated that stretched constructs cycled calcium faster than control constructs ($n = 5$/group). (D) Control constructs had longer calcium transients than stretched constructs ($n = 5$/group). (E) Quantitative real-time PCR evaluated mRNA levels of cardiac-specific ion channels from flow-sorted NKX2-5-GFP$^+$/CD90-APC$^-$ cardiomyocytes isolated from the constructs ($n = 3$/group). Data are presented as gene expression relative to the housekeeping genes GAPDH and PPIA, plotted as $2^-(\Delta C_T)$. $^*p < 0.05$, $^{**}p < 0.01$, *n.s.* = not significant.

longitudinal orientation. The proximal electrode pair was oriented on the epicardium closer to the base of the heart, while the distal electrode pair had closer proximity to the apex (Fig. 6C). APs from the construct and the myocardium occurred simultaneously, with normal frequency, and the amplitude of construct APs was smaller than those generated from the myocardium (Fig. 6D). Furthermore, the quantified ratio of AP amplitude (construct/myocardium) was significantly smaller for the stretched constructs than the control constructs (Fig. S3C; $p < 0.05$). This lower ratio suggested that the stretched constructs had better passive conduction than the acellular or control non-stretched constructs.

We also used 2D echocardiography to assess anterior wall thickness at baseline (prior to construct implantation) and at 1 and 2 weeks post-implantation (Fig. S3A). Anterior wall thickness was significantly greater in hearts implanted with stretched constructs compared to the control constructs at 2 weeks ($p < 0.05$), suggesting swelling of the implanted stretched constructs and less anterior wall thinning (Fig. S3B). Throughout the study, the surface electrocardiogram (ECG) parameters were monitored in all animals using 3-lead recordings. We observed normal ECG traces in all groups, with clearly definable P, QRS, and T waves and no noticeable abnormalities (Fig. S4A). Analysis of 5 min recordings for up to 2 weeks post-implantation revealed no differences in ECG parameters among the three groups (Fig. S4B).

Animals were sacrificed 2 weeks after construct implantation, and the hearts were rapidly excised for histological analysis. The acellular group had severe adhesions around the constructs, connecting them to the mediastinal structures, and the acellular constructs were extremely fragile and prone to tearing during the dissection. Whole-heart sections stained with Masson's trichrome (Fig. 6E), were used to measure the cross-sectional area of the constructs normalized to heart cross-sectional circumference. The stretched constructs were significantly larger than the two controls (Fig. 6F; $p < 0.05$).

The construct–epicardium interface was assessed to identify transplanted cell distribution and Gelfoam remodeling (Fig. 6G). Acellular constructs had poor contact with the epicardial surface and were densely filled with red blood cells. The Gelfoam matrix stained red, perhaps because of the red blood cells. Control constructs were more firmly attached to the epicardium than the

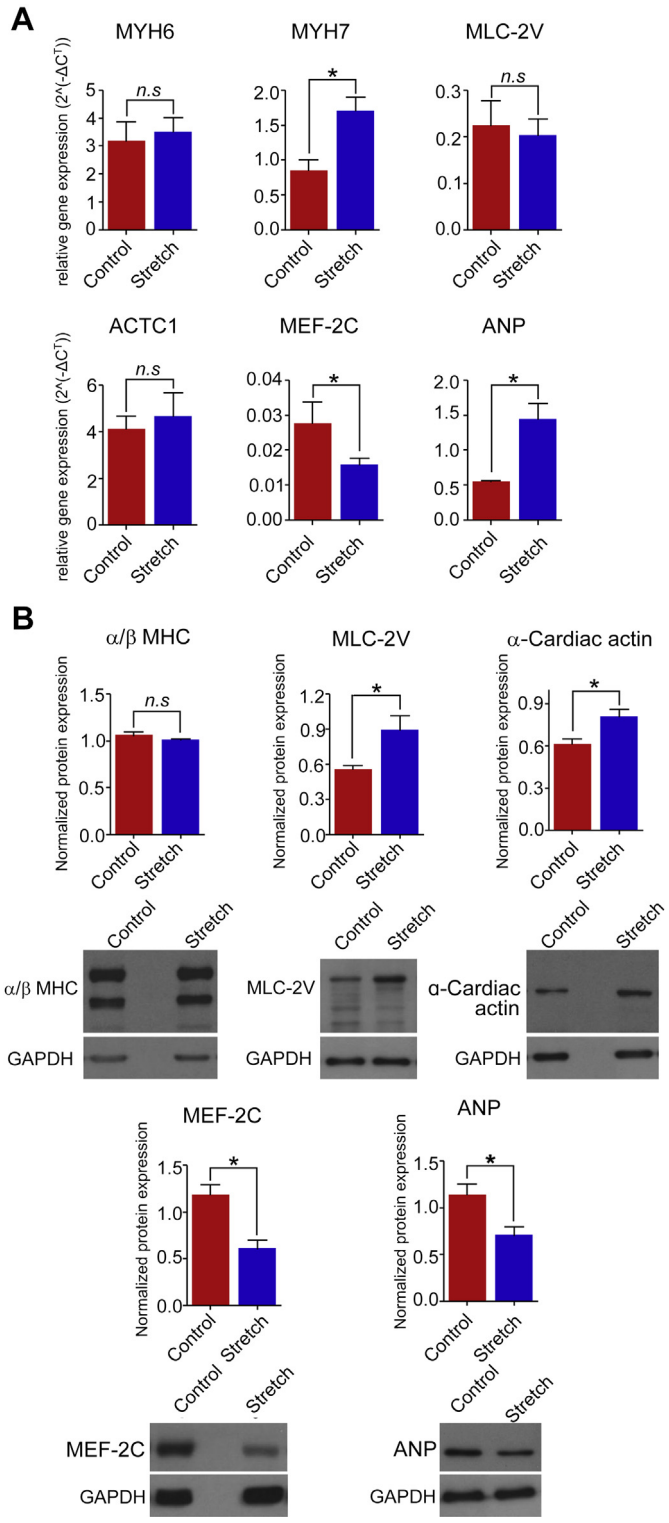

Fig. 5. Uniaxial stretching enhanced the maturation of hESC-CMs. (A) Quantitative real-time PCR evaluated mRNA levels of several genes indicative of cardiomyocyte maturity from FACS isolated NKX2.5-GFP$^+$/CD90-APC$^-$ cardiomyocytes ($n = 3$/group). Data are presented as gene expression relative to the housekeeping genes GAPDH and PPIA, plotted as $2^{-}(\Delta C_T)$. (B) Western blots of whole-cell lysates from intact scaffolds, consisting of a heterogeneous population of cells. Total combined α/β-MHC showed no difference in total protein levels; however, stretched constructs possessed significantly more MLC-2V and α-cardiac actin protein than control ($n = 3$/group). Conversely, stretched constructs had significantly less MEF-2C and ANP protein than control ($n = 3$/group). MYH6 = α-myosin heavy chain; MYH7 = β-myosin heavy chain; MLC-2V = myosin light chain 2, ventricular specific; ACTC1 = α-cardiac actin; MEF-2C = myocyte-specific enhancement factor 2C; ANP = atrial natriuretic peptide. $^*p < 0.05$, *n.s.* = not significant.

acellular constructs. Clusters of surviving cells were identified (see inset) and were dispersed into the construct to approximately 150 μm from the epicardium. However, large areas of Gelfoam remained intact with large empty porous areas, particularly at increasing distances from the epicardium. Stretched constructs were tightly attached to the epicardium and contained a higher density of cells. Elongated and striated cells were identified in the construct and penetrated more deeply, up to 500 μm from the epicardial surface. The Gelfoam matrix of stretched constructs had largely been remodeled. Finally, to confirm the presence of surviving hESC-CMs in the constructs, we stained them with an antibody for human mitochondria (Fig. 6H). Both control and stretched constructs contained cells positive for human mitochondria, while the acellular construct did not (not shown).

4. Discussion

Cell therapy to restore ventricular function after an MI may require not only cells that induce paracrine effects, but also cells that will provide new cardiomyocytes to enhance cardiac contractile force. A number of stem cells have been used for cardiac repair to generate neo-cardiomyocytes. However, research results remain controversial except for the implantation of fetal cardiomyocytes. In this study, we found that cyclic stretching helped to mature hESC-CMs in a 3D scaffold, and increased media circulation within the construct, which may have contributed to enhanced cardiomyocyte distribution in the scaffold as well as the elongation and orientation of the hESC-CMs. Cyclical stretching also increased the maturation of the hESC-CMs, which acquired a more adult-like phenotype and became a more mature beating syncytium of cardiac muscle tissue *in vitro*. This was evidenced by the faster contraction rate and shorter calcium transients, as well as stretched cells that expressed cardiac ion channels more robustly and had better coordinated myocyte contractions. *In vivo* implantation of the stretched constructs resulted in more diffuse distribution of cells in a thicker construct and may be the optimal platform for surgical repair of the damaged left ventricle.

Approximately 1 billion cardiomyocytes are required to replace those lost after an extensive MI [6]. Replacing the lost cells may require the transplantation of a large number of cells that will assume a mature cardiomyocyte phenotype. Ensuring their survival and engraftment will likely require tissue-engineered constructs.

Currently, three distinct approaches to cardiac tissue engineering have been employed with moderate pre-clinical success: (1) hydrogels or fibrin gel mixtures that provide the substrate for rapid cell attachments to a matrix; (2) multi-layered cell sheets that carry their preformed matrix when implanted on the heart; and (3) cell-seeded biodegradable scaffolds with extensive 3D matrix structures. The survival of injected cells can be increased by mixing them with fibrin gels or hydrogels [29]. However, the survival of the implanted cells remains limited even if the hydrogels are enhanced with angiogenic cytokines [30]. Cell sheets effectively maintain an extracellular matrix and support the formation of a thin syncytium of electrically integrated cardiomyocytes, while also avoiding the introduction of foreign materials to the heart [7]. They can be stacked, but their thickness is limited by oxygen and nutrient diffusion barriers given the non-porous nature of the densely seeded layers [31]. The combination of hESC-CMs and endothelial progenitor cells may improve the vascularization of the implanted cell sheets; however, even two sheets stacked together have limited thickness and can produce a limited new myocyte microtissue structure.

Three-dimensional engineered cardiac tissue constructs have been constructed using rat neonatal cardiomyocytes and cast in circular molds with collagen matrices to produce beating tissue [32]. These constructs were demonstrated to improve cardiac

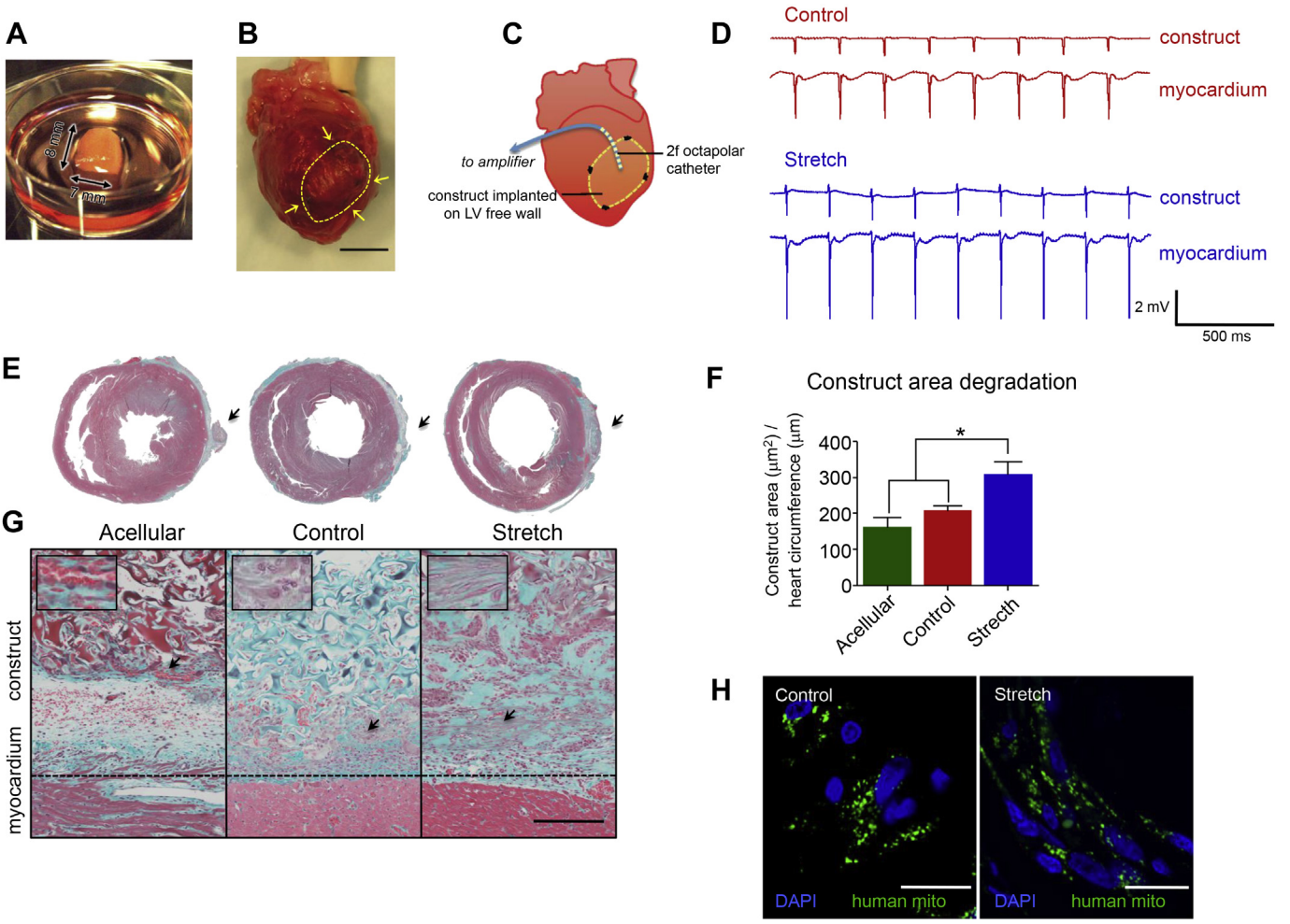

Fig. 6. Feasibility and characterization of hESC-CM–seeded constructs implanted on the epicardium in a rat I/R model. (A) Constructs measuring approximately 8 × 7 mm were surgically implanted onto the rat epicardial surface over the injured left ventricular free wall 1 week post-I/R. (B) Gross morphology of an excised rat heart 2 weeks post-implantation. The construct was clearly visible (outlined by the dashed line). Arrows indicate the position of sutures (scale bar 5 mm). (C) Schematic diagram illustrating the orientation of the 2f octapolar catheter used to make direct open-chest ECG recordings simultaneously from the native myocardium (proximal electrodes) and construct surface (distal electrodes). (D) Representative traces from control and stretched implanted constructs demonstrate the simultaneous timing of APs recorded from both the construct and myocardium. (E) Masson's trichrome staining of explanted heart cross-sections. Pink – muscle fibers, blue – collagen. Arrows indicate location of construct. (F) Construct cross-sectional area was measured and normalized to heart cross-sectional circumference. Stretched constructs had significantly larger areas than both acellular and control groups ($n = 5$/group). (G) Masson's trichrome–stained epicardial–construct interfaces demonstrated that stretched constructs underwent more Gelfoam remodeling, exhibited better cell dispersion (both near the epicardium and up to at least 500 μm), and contained more elongated cardiomyocytes (inset). Acellular constructs were torn, contained large numbers of red blood cells (inset), and the Gelfoam was stained red by coagulated blood. Control constructs contained surviving transplanted cells located close to the epicardial surface, including aggregated clusters of cells (inset), but had minimal Gelfoam remodeling. The dashed line represents the approximate location of the epicardial border (scale bar 200 μm). (H) Human mitochondrial immunofluorescence staining of control and stretched constructs revealed that transplanted cells survived for at least 2 weeks *in vivo* (scale bar 20 μm). $^{*}p < 0.05$.

function following MI in rats [33]. However, the aggregate constructs were small compared to the infarct region. We employed the FDA-approved Gelfoam scaffold, which is composed of gelatin [12,13]. This sponge-like biomaterial possesses excellent hemostatic properties and provides a suitable surface for cell attachment, avoiding cell loss due to anoikis. The addition of cytokine-entrained hydrogels injected around the scaffolds has been shown to increase angiogenesis and cell survival [34], and immobilization of proangiogenic cytokines within the scaffold provided a sustained and prolonged protein release [35]. Future generations of uniaxial stretched constructs could take advantage of the porous nature of Gelfoam and incorporate endothelial progenitor cells to establish a vascular network that could augment cell survival and angiogenesis in the scaffold *in vivo*.

Three-dimensional porous scaffolds provide a spacious and hospitable microenvironment capable of supporting cardiomyocyte maturation, which allows for the transplantation of a large number of cells with scalable scaffold dimensions. However, during *in vitro* culture and prior to the establishment of a functional capillary network for integrated vascular perfusion, construct thickness and cell survival are limited. In the current study we utilized a dynamic cell culture system employing uniaxial cyclical stretching to enhance 3D tissue formation as defined by cellular distribution and proliferation [21,36]. The cyclical stretch parameters were set to correspond to postnatal human cardiomyocytes with a stretching frequency of 1.25 Hz or 75 "beats" per minute, which is similar to the first 3 months after birth (1.7–2.5 Hz) [37]. The displacement in the uniaxial elongation of our constructs from stretched to relaxed lengths was set at 12% as previously described [24]. Finally, we assigned 37% of the duty cycle time to active stretching and the remaining 63% to relaxation of the construct, approximating a cardiac-like 1:2 duty cycle as previously reported [36,38]. With

these parameters, we observed better tissue formation, more robust cardiomyocyte composition, and increased cardiomyocyte survival similar to the initial seeding fraction (44% in stretched constructs, 26% in control). The differences could be due to enhanced survival of the cardiomyocytes in stretched constructs, the enhanced proliferation of non-cardiomyocytes in control constructs, or the death of the non-stretched cardiomyocytes due to limited oxygen and nutrient diffusion within the scaffold. We also observed more sarcomere structures in the stretched constructs. Cardiomyocytes elongate and undergo eccentric hypertrophy during development by adding sarcomere structures in series that realign as a result of mechanical stress [39].

The most appropriate combination of cells to remuscularize the infarcted ventricle has not been established. Directed differentiation of human embryonic stem cells to a beating cardiomyocyte phenotype offers the best opportunity to create a viable cardiac tissue. Using a stage-specific cytokine induction protocol, these cells can be directed toward the cardiovascular lineages and produce cardiomyocytes [25]. However, differentiated hESC-CMs are immature and have not yet acquired an adult-like phenotype [40]. Partial maturation may be desirable *in vitro* for 3D tissue formation with the hope that the final maturation will occur *in vivo*. In our study, cyclical stretch provided the cues necessary for enhanced myocyte maturation, as has been described previously in rat neonatal cardiomyocytes [32,41] and in hESC-CMs [20]. During cardiomyocyte maturation, myocytes become more closely packed and better oriented with adherent intercalated discs and gap junctions, permitting more efficient electrical and mechanical integration of the cells [42]. The plasticity of the developing cardiomyocytes facilitates the transduction of amplified electromechanical signals, altering gene expression and protein synthesis and stability, and modifying the expression of growth factors, sarcomeric proteins, ion channels, and intracellular Ca^{2+} homeostasis [43]. In our study, we observed increases in the transcript levels of β-MHC and ANP in a pure isolated population of cardiomyocytes sorted from the constructs following stretching. In contrast to transcript levels, we observed increases in total protein expression from entire constructs for MLC-2V and α-cardiac actin, while decreases were observed for MEF-2C and ANP. These results demonstrate how difficult it can be to compare the relative gene expression and protein changes in heterogeneous populations of cells comprising larger tissue structures. While we did not observe a change in the expression of α-MHC, the energy-efficient isoform that predominates during early development, we did see an increase in the β-isoform, which is more abundantly expressed in the adult heart [44]. In stretched constructs, spontaneous calcium cycling was nearly twice as fast as in control constructs. The precise mechanism responsible for the difference in pulse rate was not determined in this study and could have been the result of structural changes in the contractile apparatus, alterations in the balance of cardiac ion channels (which were observed in isolated cardiomyocytes), or better orientation and coordination of the myocyte networks linked by the enhanced expression of Cnx43. Another study investigating uniaxial stretch of hESC-CMs (3 Hz frequency) found an upregulation of both α- and β-MHC [45]. Tulloch et al. [20] reported a more than 4-fold increase in the expression of only β-MHC. The results from these studies are difficult to compare because hESC-CMs were produced using different methods and the uniaxial stretching parameters varied. In general, we observed increased gene expression in a panel of cardiac-specific ion channels and enhanced gap junction expression and calcium handling as evidenced by shorter calcium transients. Neighboring cardiomyocytes cycled calcium synchronously, at a frequency approaching the uniaxial stretching parameter (1.25 Hz). Finally, in our *in vivo* study, the transplantation of human cardiomyocytes into the rat heart limited integration as a result of the major differences in the cardiac electrical properties between these two species. Shiba et al. elegantly demonstrated the potential for electrical coupling and suppression of arrhythmias in infarcted guinea pig hearts, which have a lower intrinsic heart rate than rats, following the transplantation of hESC-CMs [46]. This study provides some suggestion for the potential clinical utility of an hESC-CM–seeded construct and supports the continued development and refinement of the platform described here. However, electrical integration of the constructs with the recipient myocardium may require additional interventions or a specially designed pacemaker.

5. Conclusions

In summary, our cyclical stretching procedure produced a high percentage of TnT-positive cells, which resulted in the formation of a 3D cardiac tissue. Despite the maturation of the hESC-CM ultrastructure, including elongation, alignment, extensive Z-banding, and the appearance of gap junctions and sarcomeres, as well as improvements in electromechanical signals, these cells still exhibited a largely fetal-like cardiomyocyte phenotype. We posit that further maturation could occur *in vivo*, augmenting the initial maturation elicited by uniaxial stretching, which might ultimately be accompanied by a loss of automaticity as hESC-CMs adopt an adult ventricular phenotype. Additional studies will be required to determine the potential of this approach.

Acknowledgments

We thank the members of the Li and Keller laboratories for helpful discussions, and Kelly Davis for assistance preparing this manuscript. RKL holds a Canada Research Chair in Cardiac Regeneration. This research was supported by grants from the Canadian Institutes of Health Research (RMF111623 and MOP119507 to RKL). AM is a recipient of a Canadian Institutes of Health Research Banting and Best Canada Doctoral Scholarship.

Appendix A. Supplementary data

Supplementary data related to this article can be found online at http://dx.doi.org/10.1016/j.biomaterials.2013.12.052

References

[1] Rane AA, Christman KL. Biomaterials for the treatment of myocardial infarction: a 5-year update. J Am Coll Cardiol 2011;58:2615–29.
[2] Brunt KR, Weisel RD, Li RK. Stem cells and regenerative medicine–future perspectives. Can J Physiol Pharmacol 2012;90:327–35.
[3] Heldman AW, Zambrano JP, Hare JM. Cell therapy for heart disease: where are we in 2011? J Am Coll Cardiol 2011;57:466–8.
[4] Blin G, Nury D, Stefanovic S, Neri T, Guillevic O, Brinon B, et al. A purified population of multipotent cardiovascular progenitors derived from primate pluripotent stem cells engrafts in postmyocardial infarcted nonhuman primates. J Clin Invest 2010;120:1125–39.
[5] Zvibel I, Smets F, Soriano H. Anoikis: roadblock to cell transplantation? Cell Transplant 2002;11:621–30.
[6] Robey TE, Saiget MK, Reinecke H, Murry CE. Systems approaches to preventing transplanted cell death in cardiac repair. J Mol Cell Cardiol 2008;45:567–81.
[7] Bel A, Planat-Bernard V, Saito A, Bonnevie L, Bellamy V, Sabbah L, et al. Composite cell sheets: a further step toward safe and effective myocardial regeneration by cardiac progenitors derived from embryonic stem cells. Circulation 2010;122:S118–23.
[8] Kutschka I, Chen IY, Kofidis T, Arai T, von Degenfeld G, Sheikh AY, et al. Collagen matrices enhance survival of transplanted cardiomyoblasts and contribute to functional improvement of ischemic rat hearts. Circulation 2006;114:I167–73.
[9] Madden LR, Mortisen DJ, Sussman EM, Dupras SK, Fugate JA, Cuy JL, et al. Proangiogenic scaffolds as functional templates for cardiac tissue engineering. Proc Natl Acad Sci U S A 2010;107:15211–6.
[10] Hamdi H, Furuta A, Bellamy V, Bel A, Puymirat E, Peyrard S, et al. Cell delivery: intramyocardial injections or epicardial deposition? A head-to-head comparison. Ann Thorac Surg 2009;87:1196–203.

[11] Ozawa T, Mickle DA, Weisel RD, Koyama N, Ozawa S, Li RK. Optimal biomaterial for creation of autologous cardiac grafts. Circulation 2002;106:I176–82.
[12] Sakai T, Li RK, Weisel RD, Mickle DA, Kim ET, Jia ZQ, et al. The fate of a tissue-engineered cardiac graft in the right ventricular outflow tract of the rat. J Thorac Cardiovasc Surg 2001;121:932–42.
[13] Li RK, Jia ZQ, Weisel RD, Mickle DA, Choi A, Yau TM. Survival and function of bioengineered cardiac grafts. Circulation 1999;100:II63–9.
[14] Adler ED, Chen VC, Bystrup A, Kaplan AD, Giovannone S, Briley-Saebo K, et al. The cardiomyocyte lineage is critical for optimization of stem cell therapy in a mouse model of myocardial infarction. FASEB J 2010;24:1073–81.
[15] Pillekamp F, Haustein M, Khalil M, Emmelheinz M, Nazzal R, Adelmann R, et al. Contractile properties of early human embryonic stem cell-derived cardiomyocytes: beta-adrenergic stimulation induces positive chronotropy and lusitropy but not inotropy. Stem Cells Dev 2012;21:2111–21.
[16] Chen HS, Kim C, Mercola M. Electrophysiological challenges of cell-based myocardial repair. Circulation 2009;120:2496–508.
[17] Boudou T, Legant WR, Mu A, Borochin MA, Thavandiran N, Radisic M, et al. A microfabricated platform to measure and manipulate the mechanics of engineered cardiac microtissues. Tissue Eng Part A 2012;18:910–9.
[18] Heidi Au HT, Cui B, Chu ZE, Veres T, Radisic M. Cell culture chips for simultaneous application of topographical and electrical cues enhance phenotype of cardiomyocytes. Lab Chip 2009;9:564–75.
[19] Radisic M, Park H, Shing H, Consi T, Schoen FJ, Langer R, et al. Functional assembly of engineered myocardium by electrical stimulation of cardiac myocytes cultured on scaffolds. Proc Natl Acad Sci U S A 2004;101:18129–34.
[20] Tulloch NL, Muskheli V, Razumova MV, Korte FS, Regnier M, Hauch KD, et al. Growth of engineered human myocardium with mechanical loading and vascular coculture. Circ Res 2011;109:47–59.
[21] Akhyari P, Fedak PW, Weisel RD, Lee TY, Verma S, Mickle DA, et al. Mechanical stretch regimen enhances the formation of bioengineered autologous cardiac muscle grafts. Circulation 2002;106:I137–42.
[22] Kensah G, Gruh I, Viering J, Schumann H, Dahlmann J, Meyer H, et al. A novel miniaturized multimodal bioreactor for continuous in situ assessment of bioartificial cardiac tissue during stimulation and maturation. Tissue Eng Part C Methods 2011;17:463–73.
[23] Bhana B, Iyer RK, Chen WL, Zhao R, Sider KL, Likhitpanichkul M, et al. Influence of substrate stiffness on the phenotype of heart cells. Biotechnol Bioeng 2010;105:1148–60.
[24] Pang Q, Zu JW, Siu GM, Li RK. Design and development of a novel biostretch apparatus for tissue engineering. J Biomech Eng 2010;132:014503.
[25] Yang L, Soonpaa MH, Adler ED, Roepke TK, Kattman SJ, Kennedy M, et al. Human cardiovascular progenitor cells develop from a KDR+ embryonic-stem-cell-derived population. Nature 2008;453:524–8.
[26] Kattman SJ, Witty AD, Gagliardi M, Dubois NC, Niapour M, Hotta A, et al. Stage-specific optimization of activin/nodal and BMP signaling promotes cardiac differentiation of mouse and human pluripotent stem cell lines. Cell Stem Cell 2011;8:228–40.
[27] El-Mounayri O, Mihic A, Shikatani EA, Gagliardi M, Steinbach SK, Dubois N, et al. Serum-free differentiation of functional human coronary-like vascular smooth muscle cells from embryonic stem cells. Cardiovasc Res 2013;98:125–35.
[28] Dubois NC, Craft AM, Sharma P, Elliott DA, Stanley EG, Elefanty AG, et al. SIRPA is a specific cell-surface marker for isolating cardiomyocytes derived from human pluripotent stem cells. Nat Biotechnol 2011;29:1011–8.
[29] Chung JC, Mihic A, Weisel RD, Li RK. Injectable scaffolds for cardiac regeneration. In: Wang P, Kuo CH, Takeda N, Singal PK, editors. Adaptation biology and medicine. Cell adaptations and challenges, vol. 6. New Delhi, India: Narosa Publishing House Pvt. Ltd; 2011. pp. 1–15.
[30] Wu J, Zeng F, Huang XP, Chung JC, Konecny F, Weisel RD, et al. Infarct stabilization and cardiac repair with a VEGF-conjugated, injectable hydrogel. Biomaterials 2011;32:579–86.
[31] Radisic M, Yang L, Boublik J, Cohen RJ, Langer R, Freed LE, et al. Medium perfusion enables engineering of compact and contractile cardiac tissue. Am J Physiol Heart Circ Physiol 2004;286:H507–16.
[32] Zimmermann WH, Schneiderbanger K, Schubert P, Didie M, Munzel F, Heubach JF, et al. Tissue engineering of a differentiated cardiac muscle construct. Circ Res 2002;90:223–30.
[33] Zimmermann WH, Melnychenko I, Wasmeier G, Didie M, Naito H, Nixdorff U, et al. Engineered heart tissue grafts improve systolic and diastolic function in infarcted rat hearts. Nat Med 2006;12:452–8.
[34] Miyagi Y, Zeng F, Huang XP, Foltz WD, Wu J, Mihic A, et al. Surgical ventricular restoration with a cell- and cytokine-seeded biodegradable scaffold. Biomaterials 2010;31:7684–94.
[35] Kang K, Sun L, Xiao Y, Li SH, Wu J, Guo J, et al. Aged human cells rejuvenated by cytokine enhancement of biomaterials for surgical ventricular restoration. J Am Coll Cardiol 2012;60:2237–49.
[36] Pang Q, Zu JW, Siu GM, Li RK. A uniaxial cyclic stretch apparatus affected cell proliferation and cell orientation. Int J Biomechatronics Biomedical Robot 2010;1:79–87.
[37] Bernstein D. History and physical evaluation. In: Kliegman RM, Behrman RE, Jenson HB, Stanton BF, editors. Nelson textbook of pediatrics. 18th ed. Philadelphia, Pa: Saunders Elsevier; 2007. Chap. 422.
[38] Murry CE, Wiseman RW, Schwartz SM, Hauschka SD. Skeletal myoblast transplantation for repair of myocardial necrosis. J Clin Invest 1996;98:2512–23.
[39] Russell B, Curtis MW, Koshman YE, Samarel AM. Mechanical stress-induced sarcomere assembly for cardiac muscle growth in length and width. J Mol Cell Cardiol 2010;48:817–23.
[40] Liu J, Fu JD, Siu CW, Li RA. Functional sarcoplasmic reticulum for calcium handling of human embryonic stem cell-derived cardiomyocytes: insights for driven maturation. Stem Cells 2007;25:3038–44.
[41] Tiburcy M, Didie M, Boy O, Christalla P, Doker S, Naito H, et al. Terminal differentiation, advanced organotypic maturation, and modeling of hypertrophic growth in engineered heart tissue. Circ Res 2011;109:1105–14.
[42] Peters NS, Severs NJ, Rothery SM, Lincoln C, Yacoub MH, Green CR. Spatiotemporal relation between gap junctions and fascia adherens junctions during postnatal development of human ventricular myocardium. Circulation 1994;90:713–25.
[43] Sadoshima J, Izumo S. The cellular and molecular response of cardiac myocytes to mechanical stress. Annu Rev Physiol 1997;59:551–71.
[44] Miyata S, Minobe W, Bristow MR, Leinwand LA. Myosin heavy chain isoform expression in the failing and nonfailing human heart. Circ Res 2000;86:386–90.
[45] Shimko VF, Claycomb WC. Effect of mechanical loading on three-dimensional cultures of embryonic stem cell-derived cardiomyocytes. Tissue Eng Part A 2008;14:49–58.
[46] Shiba Y, Fernandes S, Zhu WZ, Filice D, Muskheli V, Kim J, et al. Human ES-cell-derived cardiomyocytes electrically couple and suppress arrhythmias in injured hearts. Nature 2012;489:322–5.